CORROSION SCIENCE AND TECHNOLOGY, Vol.7, No.3(2008), pp.152~157

Corrosion Mechanisms of New Wrought Mg-Zn Based Alloys Alloying with Si, Ca and Ag

G. Ben-Hamu[1], D. Eliezer[1,†], K.S. Shin[2], and L.Wagner[3]

[1]*Department of Materials Engineering, Ben-Gurion University of the Negev, Beer-Sheva 84105, Israel*
[2]*Department of Materials Science and Engineering, Magnesium Technology Innovation Center, Seoul National University, Seoul 151-744, South Korea*
[3]*Institute of Materials Science and Engineering, TU Clausthal, Germany*

New wrought magnesium alloys have increasingly been developed in recent years for the automotive industry due to their high potential as structural materials for low density and high strength/weight ratio demands. However, their poor mechanical properties and low corrosion resistance have led to a search for new kinds of magnesium alloys with better strength, ductility, and high corrosion resistance. The main objective of this research is to investigate the corrosion behaviour of new magnesium alloys: Mg-Zn-Ag (ZQ), Mg-Zn-Mn-Si (ZSM) and Mg-Zn-Mn-Si-Ca (ZSMX). These ZQ6X, ZSM6X1, and ZSM651+YCa alloys were prepared using hot extrusion. AC, DC polarization and immersion tests were carried out on the extruded rods. Microstructure was examined using optical and electron microscopy (SEM) and EDS. The addition of silver decreased the corrosion resistance. The additions of silicon and calcium also affected the corrosion behaviour. These results can be explained by the effects of alloying elements on the microstructure of Mg-Zn alloys such as grain size and precipitates caused by the change in precipitation and recrystallisation behaviour.

Keywords *: Mg-Zn alloys, corrosion behaviour, hot extrusion method, electrochemical techniques*

1. Introduction

The interest in lightweight materials in structural applications has increased significantly due to their importance in environmental and energy saving problems. Especially in the automotive industry, magnesium alloys, due to their low density and high specific strength, have become the key materials for enhancing fuel efficiency. In fact, there has been a rapid growth in the structural applications of magnesium alloys during the past decade. However, the majority of this growth has been in the area of die-cast components and some semi-solid formed components.[1)] In contrast, wrought magnesium alloys are used for approximately only 1% of total magnesium consumption. There are two major technical issues in expanding the wrought magnesium market. The first is the low production rate. A typical magnesium alloy must be extruded 5-10 times slower than a typical aluminium alloy. The second is development of new wrought magnesium alloys with a combination of high strength, high ductility, and high corrosion resistance.

In recent years, modification of alloy composition and/or heat treatment has been attempted for improved mechanical properties[2)-4)] and corrosion resistance[5)-8)] in the casting alloys. However, there is a growing need for high strength wrought Mg alloys in the automotive and aerospace industries. Four different alloy systems have mainly been utilized for the development of the wrought Mg alloys, i.e., Mg-Zn, Mg-Al, Mg-Th, and Mg-Mn alloys.[9)] Among these, Mg-Zn alloys were found to have a large age hardening response stemming from the precipitation of a transition phase (β'), and consequently offered a combination of good strength and ductility.[10),11)] It has been reported, however, that grain refinement is difficult to achieve in Mg-Zn alloys.[9)] Several alloying elements, including Zr, rare-earth (RE), and Cu, have been added to Mg-Zn alloys to improve the mechanical properties; Zr for grain refining and strengthening,[12)] RE for improved high temperature properties,[13)] and Cu for ductility improvement.[14)]

Mg-Zn-Si series is a new promising alloy system developed to meet the above requirements. The silicon addition to magnesium alloys causes an increased fluidity of the molten metal. The Mg_2Si formed by the addition of Si exhibits high melting point (1085℃), high hardness (460 $HV_{0.3}$), low density (1.9 g cm^{-3}), high elastic modulus (120 GPa), and low thermal expansion coefficient (7.5×10^{-6}

† Corresponding author: deliezer@bgu.ac.il

K^{-1}).[15] This intermetallic phase is very stable and can impede grain boundary sliding at elevated temperatures. Guangyin et al.[16] investigated the microstructural features, tensile properties at both ambient and elevated temperature of 150℃, impact toughness, and creep resistance to get a better overall understanding of alloys in this system. They identified the most promising compositions as those of Mg?Zn?Si alloyed with Ca. But up to now, limited research has been carried out on the electrochemical behaviour of this system. The objective of the present study is to develop new wrought Mg alloys with improved strength and ductility and investigate the corrosion resistance of the new alloys. The effects of Ag or Si and Ca addition of the new Mg-Zn-Ag, Mg-Zn-Mn-Si, and Mg-Zn-Mn-Si-Ca alloys were examined.

2. Experimental procedures

Mg-Zn alloys were melted in a low carbon steel crucible and melt surface was protected with a gas mixture of CO_2+0.5% SF_6. The alloying elements Zn, Ag, Ca, and Mn with 99.99% purity were added to the melt. Silicon was added to the melt in the form of Mg-10 wt% Si mother alloy. The alloy designations used in the present study are listed in Table 1. The ingots were homogenized at 400℃, water-cooled, and subsequently scalped to give 80 mm diameter billets. After preheating, the billets were extruded at 350℃ and 300℃ for ZQ6X and ZS6X, respectively, with an extrusion ratio of 25:1 to give 16 mm diameter cylindrical rods.

Specimens for optical microscopy were mechanically polished followed by chemical etching with a 1% HNOs + 24% distilled water + 75% diethylene glycol solution.

Table 1. Chemical composition of the extruded Mg-Zn alloys (in wt.%)

Alloy	Zn	Ag	Mn	Si	Ca
ZQ60	6	0	-	-	-
ZQ61	6	1	-	-	-
ZQ62	6	2	-	-	-
ZQ63	6	3	-	-	-
ZM60	6	-	0.5	0	-
ZSM600	6	-	0.5	0.5	-
ZSM610	6	-	0.5	1	-
ZSM620	6	-	0.5	2	-
ZSM651+0.4Ca	6	-	1	5	0.4
ZSM651+0.6Ca	6	-	1	5	0.6
ZSM651+0.8Ca	6	-	1	5	0.8

The electrochemical behaviour of both Mg-Zn-Ag, Mg-Zn-Mn-Si, and Mg-Zn-Mn-Si-Ca magnesium alloys was investigated using linear polarization (LP) measurements (DC polarization) and Electrochemical Impedance Spectroscopy (EIS). All the electrochemical measurements were performed in 3.5% NaCl saturated with $Mg(OH)_2$ with a pH = 10.5 at which Mg can cover itself with more or less protective oxide or hydroxide which checks the dissolution reaction.[17] The electrochemical testing was employed to study the main features of the processes taking place at the alloy/solution interface. The effect of alloying elements on the Mg-Zn alloys' corrosion resistance was studied. The corrosion resistance of Mg alloys was pointed out by EIS measurements performed during the free immersion time and the effect of the different alloying elements was studied. The behaviour of the electrode/electrolyte interface at different immersion times was also studied. Corrosion rates were derived from polarization data by the common method.[18] For all measurements a three-electrode electrochemical cell was used, with an SCE as reference electrode and a platinum counter electrode. The working electrode was prepared from the Mg-alloy samples embedded in an acrylic resin to provide electrical isolation of the sample surface. The samples were air dried at room temperature. The linear curves were obtained using a 273A EG&G Potentiostat/Galvanostat, with a voltage scan rate of 0.5 mV/s. The impedance measurements were carried out using a PARSTAT 2263 frequency response analyser coupled with the potentiostat. All the experiments were controlled by a PC, which was also used for the collection, storage, and plotting of data. The scanned frequency ranged from 6 mHz to 100 kHz and the perturbation amplitude was 5 mV (it was observed that a variation of the amplitude did not change the frequency response of the electrode/electrolyte interface). The impedance measurements were performed at open circuit potential (E_{oc}). A partial data fitting made with the Boukamp circuit equivalent software[19] for the charge transfer process produced the R_p (polarization resistance) and C_{dl} (double-layer capacitance) values.

For constant immersion testing, the specimens were cleaned with alcohol, acetone, and distilled water. The cleaned samples prior to weighing were exposed to the solution (500 ml 3.5% NaCl saturated with $Mg(OH)_2$) for 72 h. At the end of the experiment, cleaning of specimens was carried out by dipping in a solution of 30% CrO_3 in 100 ml distilled water under boiling conditions. The weight loss was measured after each experiment and the corrosion rate was calculated in mpy. The specimens were weighed on an analytical balance to an accuracy of ±0.1 mg, and the specimens were photographed before and after

removing their corrosion products.

3. Results and discussion

3.1 Microstructure of the extrusions alloys:

The decrease in grain size with increasing silver content in the alloy is shown in Fig. 1. The average grain size of the alloy with no silver is larger, about 20 μm, and the precipitate density is rather low compared to the alloys containing silver. Relatively few and coarser precipitates decorate the grain boundaries and the grain interiors appear to contain finer precipitates in the alloy free of silver. The precipitate density, both on the grain boundaries and within the grains, increases considerably with increasing silver content while the average grain size decreases. As can be seen from the SEM images in Fig. 1, the average grain size decreases to about 10 μm with 1% Ag and to about 5 μm with 2% Ag additions, while the grain size is no longer discernible in the alloy with 3% Ag addition due to densely populated precipitates.

The microstructure of the as-extruded ZM60, ZSM600, ZSM610, and ZSM620 alloys is shown in Fig. 2. The average grain sizes of the extruded ZSM alloys were 23 μm, 12.1 μm, 11.3 μm, and 10.3 μm, respectively. As shown in the SEM analysis in Fig. 3, fine Mg_2Si phases are distributed parallel to the extrusion direction in the ZSM610 alloy. Also, the type of the Mg_2Si particles was polygonal script. Therefore, the grain refinement of the Mg-Zn-Mn-Si alloy can be explained as grain growth which is suppressed by the formation of precipitates containing Mg and Si during recrystallization. The Mg_2Si polygon was created by breakage of the Chinese type Mg_2Si during the extrusion process. The polygonal type Mg_2Si phases are dispersed parallel to the extrusion direction in the as-extruded ZSM alloys.

The microstructures of the ZSM651 + 0.4Ca, ZSM651 + 0.6Ca, and ZSM651 + 0.8Ca alloys in the as-extruded condition are shown in Fig. 4. From these microstructures, it can be seen that the addition of Si suppressed grain growth during the extrusion process. It can be observed that the $MgZn_2$ phase appears as clusters of small particles, which are aligned in the extrusion direction. The latter morphology is probably caused by the extrusion process that fractures the intermetallic. The Mg_2Si, Mn_5Si_3 and CaMgSi intermetallics often have polygonal shape.

3.2 Corrosion behaviour of the extrusion alloys

Immersion tests were used in this work in order to understand the effects of Ag addition on corrosion resistance. The effects of silver on the corrosion rates of the ZQ6x

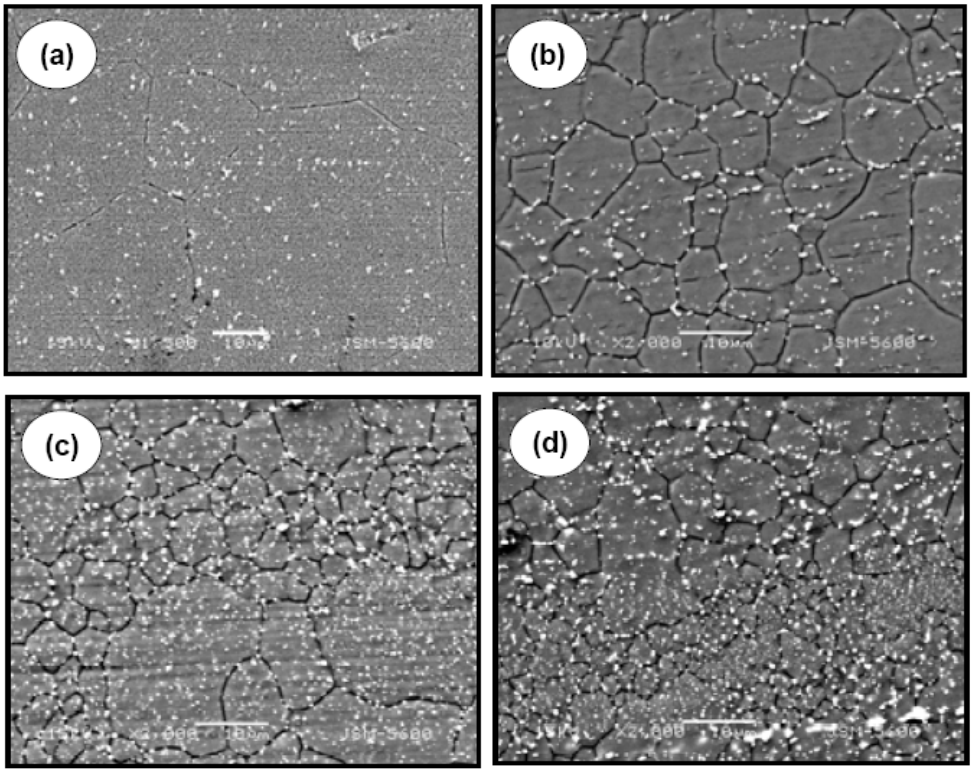

Fig. 1. The influence of the silver addition on the microstructure. (a) ZQ60; (b) ZQ61; (c) ZQ62; (d) ZQ63.

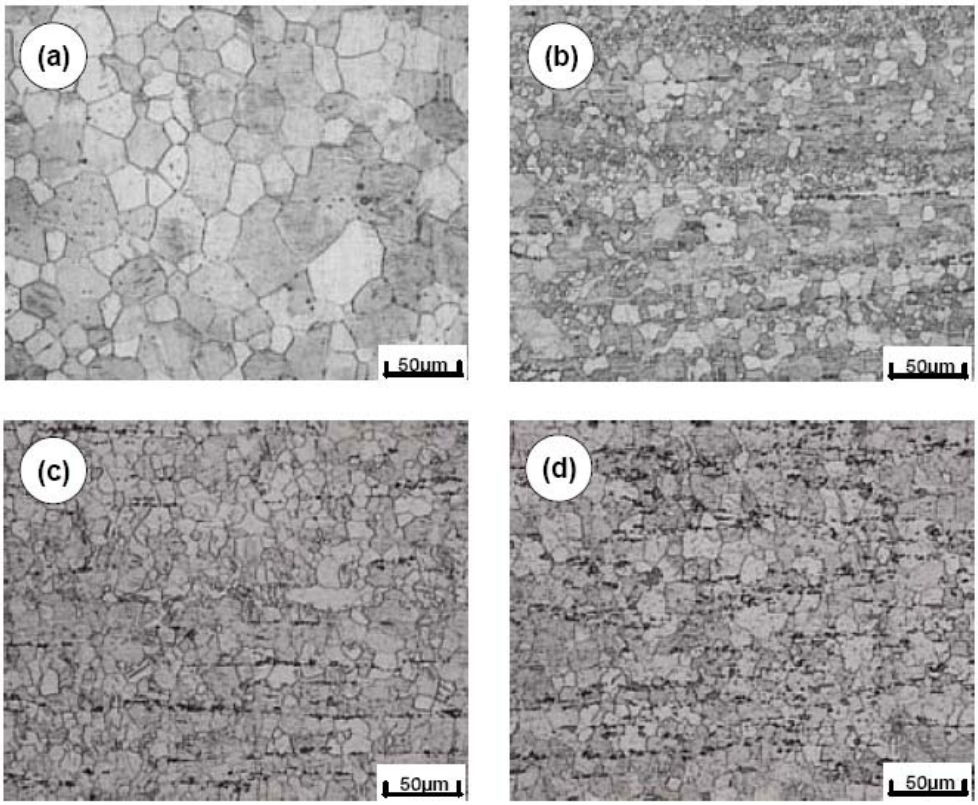

Fig. 2. Typical microstructure of extruded Mg alloys; (a) ZM60, (b) ZSM600, (c) ZSM610 and (d) ZSM620.

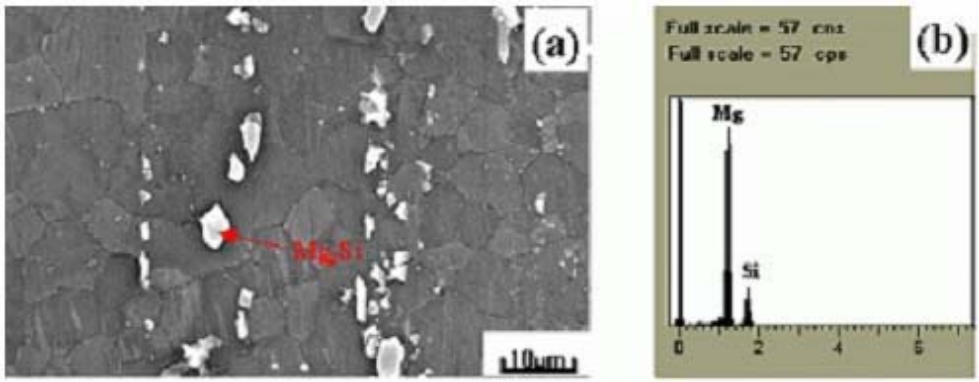

Fig. 3. SEM micrograph of the as-extruded ZSM610 alloy; (a) SEM micrograph and (b) the result of EDS analysis.

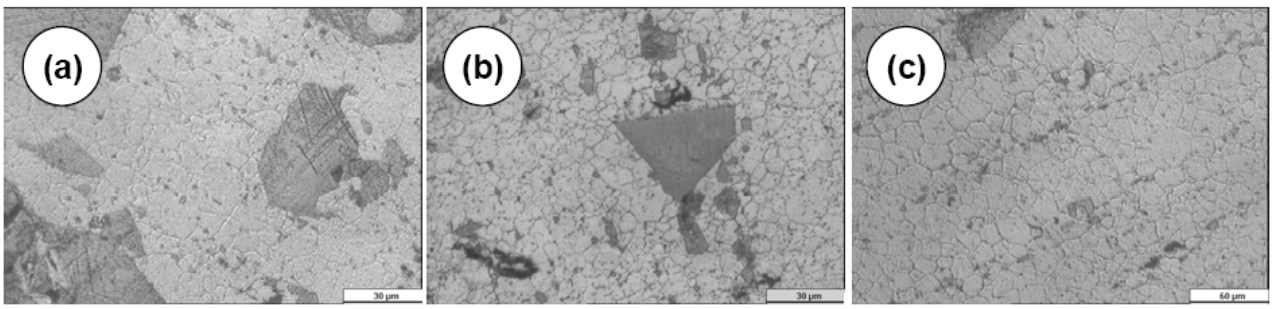

Fig. 4. Typical microstructure of extruded Mg alloys; (a) ZSM651+0.4Ca, (b) ZSM651+0.6Ca and (c) ZSM651+0.8Ca.

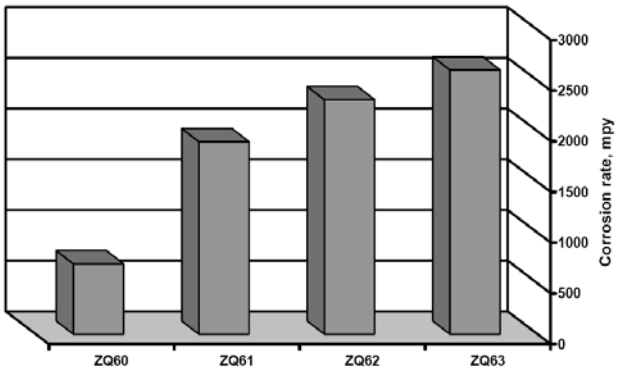

Fig. 5. The effects of silver addition on the corrosion rates of the ZQ6x alloys.

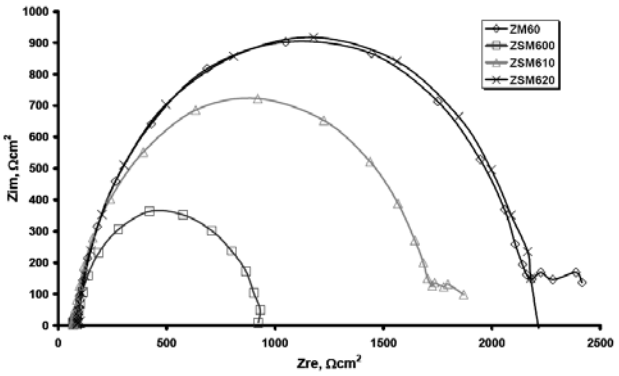

Fig. 6. Nyquist plot at free immersion potential for ZSM6X1 magnesium alloys.

alloys are shown in Fig. 5. The addition of silver to the Mg-Zn alloys increased the corrosion rates of the extrusions compared to those of the ZQ60 alloy. This increase in corrosion rate by Ag addition to the Mg-6%Zn alloy is considered to be caused by the formation of a micro-galvanic cell between the α-Mg (solid solution) and the precipitates of Mg-Ag ($Mg_{54}Ag_{17}$) due to their different electrochemical potentials.[20] The Nyquist plots of Mg-Zn-Mn alloys containing different quantities of Si at open circuit exhibit one capacitive loop (Fig. 6).

The Nyquist diagrams obtained at the potential of open circuit present a capacitive loop at high and intermediate frequencies. In addition, at low frequencies a small capacitive loop was always observed for two of the samples (ZM60 and ZSM610), this loop being more or less reproducible. The EIS data for the first capacitive loop associated at the transfer charge process can be fitted with the Boukamp circuit equivalent,[18] the equivalent circuit consisting of a R_p and a C_{ld} in parallel.

The obtained $1/R_p$ (which is proportional to the corrosion rate) is plotted as a function of Si contents (Fig. 9), for ZSM6*X0* alloys. Moreover, the corrosion rate values de-

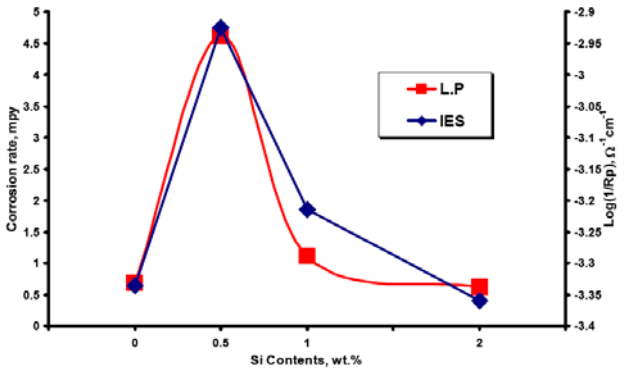

Fig. 7. Corrosion rate (~$1/R_p$) from EIS measurements and corrosion rate from linear polarization as function of Si contents for ZSM6X1 magnesium alloys.

termined on the linear polarization curves (DC measurements) are regrouped in Fig. 7. It can be seen that the maximal $1/R_p$ value is obtained for the alloys containing 0.5 wt% of Si (ZSM600). Thus, the $1/R_p$ values obtained on the EIS measurements pass over the maximum increase in Si contents, in the same way as the corrosion current determined on the DC polarization.

It is known that silicon has little deleterious effect on the basic salt-water corrosion performance of pure magnesium because the electrochemical potential of the Mg_2Si precipitate (-1.65 V_{SCE}) is similar to that of magnesium (-1.66 V_{SCE}). However, the corrosion behaviour of ZS6*X*-extruded magnesium alloys is influenced by the size and the quantity of Mg_2Si particles. The Mg_2Si phase plays a dual role, depending on its volume fraction ($f = V_{Mg2Si}/V_a$) in the microstructure. As f increased (from Chinese Script Type in ZSM600 to Polygonal type in ZSM620-Fig. 2) the corrosion resistance increased also. Moreover, Si additions may affect the corrosion behaviour by surface oxidation.[21]

The potentiodynamic curves obtained for Mg-Zn-Mn-Si containing different quantities of Ca alloys as a function of Ca contents are shown in Fig. 8. The effect of the alloying element (Ca) on the corrosion behaviour can be seen. The corrosion parameters estimate the effect of the alloying element, which means increasing the anodic current densities and the disennobeling of the potential values.

The effect of calcium on the corrosion rate of the ZSM651 alloy is shown in Fig. 9. As shown in this Fig., the addition of calcium increases the corrosion rates of the ZSM651+YCa alloys.

High Ca content (Si content is constant) increases the quantity and size of the CaMgSi phase. This phase has a potential difference higher than the magnesium matrix.[21] A high quantity of CaMgSi at the surface creates more microgalvanic sites. Therefore, high Ca content in Mg-Zn-

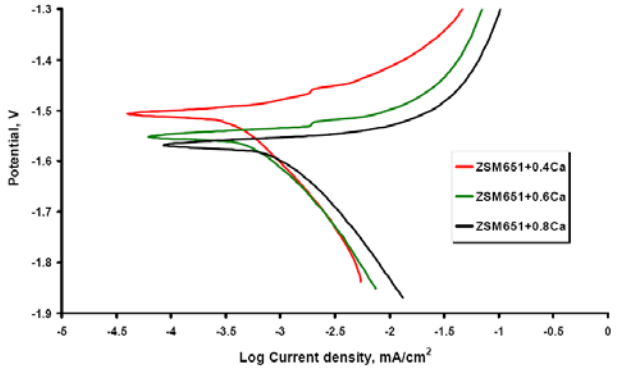

Fig. 8. Potentiodynamic curves of ZSM651+*y*Ca (y=0.4,0.6,0.8 wt%) Mg alloys in 3.5% NaCl saturated with $Mg(OH)_2$.

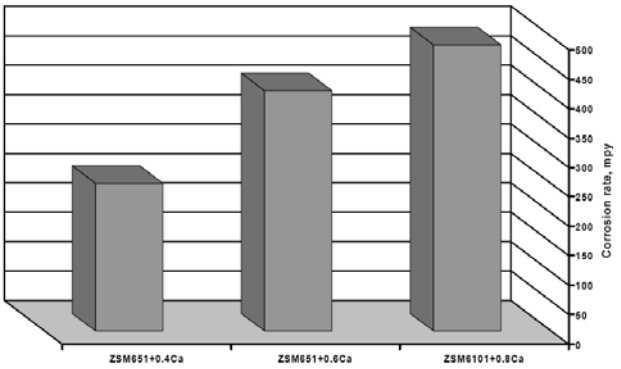

Fig. 9. Corrosion rate (potentiodynamic polarization methods) of ZSM651+YCa Mg alloys in 3.5% NaCl saturated with $Mg(OH)_2$.

Mn-Si alloy decreases the corrosion resistance.

4. Summary

1) The grain size of the Mg-6%Zn alloy was significantly refined with the addition of silver or silicon and calcium in the as-extruded condition.

2) Addition of silver decreased the corrosion resistance: This increase in corrosion rate by addition of Ag to the Mg-Zn alloy is considered to be caused by the formation of a micro-galvanic cell between the α-Mg (solid solution) and the precipitates of Mg-Ag ($Mg_{54}Ag_{17}$) due to their different electrochemical potentials.

3) The addition of silicon decreased the corrosion rates of the ZSM6*X*1 alloys. It is known that silicon has little deleterious effect on the basic salt-water corrosion performance of pure magnesium because the electrochemical potential of the Mg_2Si precipitate (-1.65 V.SCE) is similar to that of magnesium (-1.66 V.SCE).

4) The addition of calcium to the Mg-6% Zn-1% Mn-5% Si alloy decreased the corrosion resistance. Due to the formation of cathodic sites between the magnesium matrix and the CaMgSi intermetallics.

References

1. C. D. Yim and K. S. Shin, *Mater. Trans*., **44**, 558 (2003).
2. D. H. Kim, S. J. Song, H. Park, and K. S. Shin, *Met. Mater*., **3**, 51 (1997).
3. J. W. Kim, D. H. Kim, C. D. Yim, and K. S. Shin, *J. Kor. Inst. Met. Mater*., **35**, 1446 (1997).
4. J. J. Kim, D. H. Kim, K. S. Shin, and N. J. Kim, *Scripta mater*., 1999, **41**, 333.
5. C. D. Lee, C. S. Kang, and K. S. Shin, *Met. Mater*., **6**, 351 (2000).
6. C. D. Lee, C. S. Kang, and K. S. Shin, *Met. Mater*., **6**, 441 (2000).
7. C. D. Lee, C. S. Kang, and K. S. Shin, *Met. Mater.-Int*., **7**, 296 (2001).
8. Y. J. Ko, C. D. Yim, J. D. Lim, and K.S. Shin, *Mater. Sci. Forum*, **419**, 851 (2003).
9. C. S. Roberts, Magnesium and Its Alloys, John Wiley & Sons, New York, 1960.
10. L. Sturkey and J. B. Clark, *J. Inst. Met.*, **88**, 177 (1959-60).
11. J. B. Clar, *Acta. Metall*., **13**, 1281 (1965).
12. A. K. Bhambri and T. Z. Kattamis, *Metall. Trans*., **2**, 1869 (1971).
13. V. Sustek, S. Spigarelli, and J. Cadek, *Scripta mater*., **35**, 449 (1996).
14. W. Unsworth and J. F. King, Magnesium Technology, p. 25, The Inst. of Metal, 1987.
15. S. Beer, G. Frommeyer, and E. Schmid, *Proceedings of Conference on 'Magnesium alloys and their applications'*, p. 317, Oberursel (1992).
16. Y. Guangyin, L. Manping, D. Wenjiang, and A. Inou, *Mater. Sci. Eng*., **A357**, 314320 (2003).
17. M. Pourbaix: Atlas of Electrochemical Equilibria in Aqueous Solutions, p. 141, Brussels, 1974.
18. Boukamp, Equivalent Circuit Software, Users Manual, p. 6, The Netherlands University of Twente, 1988.
19. H. H. Uhlig, Corrosion and Corrosion Control, John Wiley & Sons, New York, 1963.
20. G. Ben-Hamu, D. Eliezer, A. Kaya, Y. G. Na, and K. S. Shin, *Materials Science and Engineering A*, **435**, 579 (2006).
21. G. Ben-Hamu, D. Eliezer, and K. S. Shin, *Materials Science and Engineering A 447*, **1**, 35 (1007).